Available online at www.sciencedirect.com

ScienceDirect

Procedia Engineering 2 (2010) 2161–2169

Procedia Engineering

www.elsevier.com/locate/procedia

Fatigue 2010

# Rolling contact fatigue of railways wheels: influence of steel grade and sliding conditions

J-F. Brunel[a], E. Charkaluk[a,]*, P. Dufrénoy[a], F. Demilly[b]

[a] *Laboratoire de Mécanique de Lille – UMR CNRS 8107, Cité Scientifique, 59655 Villeneuve d'Ascq, France*
[b] *GHH-Valdunes, BP12, 59125 Trith Saint Léger, France*

Received 8 March 2010; revised 9 March 2010; accepted 15 March 2010

**Abstract**

The aim of this work is to develop a numerical approach which is able to compare the different steel grades influence on rolling contact fatigue of railways wheels according to practical conditions. The main stages are the identification of the material behavior, the determination of the stress-strain fields and the application of a fatigue criterion. Two steels usually used for the manufacturing of wheels have been studied, R9T and 50CrMo4. Their influence has been numerically studied. Results show that the threshold of elastic and plastic shakedown differs depending on the steel grades and consequently the risk of damage can be affected. This methodology allows a classification of the material grades face the risk on rolling contact fatigue.



*Keywords:* rolling contact fatigue; shakedown; steady-state algorithm; plasticity

## 1. Introduction

With the increase of train speeds and axle loads, rolling contact fatigue of railway wheels has become an important issue with respect to failure. Three types of fatigue in wheels are accounted for: surface and subsurface initiated fatigue and cracking initiated at deep material defects. With the increase of the material process quality, the last one rarely appends. Surface and subsurface fatigue differ according mainly to loading intensity and sliding at the wheel rail contact. Even if simplified models, like the shakedown map (see figure 1), may be used to analyze and to classify the cases of surface fatigue [1], such approaches are not sufficiently precise to compare different steel grades. The choice of steel grades or heat treatment is very important for wheel manufacturers face the risk of rolling contact fatigue. These choices have to be optimized face the loading conditions. Two steels usually used for the manufacturing of wheels have been studied in the present work: R9T and 50CrMo4.

The aim of this work is to develop a numerical approach which is able to compare the different steel grades influence according to practical conditions. The main stages are the identification of the material behavior, the determination of the stress-strain fields and the application of a fatigue criterion.

* Corresponding author.
*E-mail address*: eric.charkaluk@ec-lille.fr

1877-7058 
doi:10.1016/j.proeng.2010.03.232

By considering the cyclic stress-strain curve for the different steels, the Armstrong-Frederick plastic model with a non linear kinematic hardening law has been chosen and the identification of the parameters has been realized from the cyclic mechanical tests.

Local stress and strain responses on the wheel have been calculated using a eulerian description of the wheel-rail contact in order to limit the size of the finite element model [2]. Computations have been performed with the Abaqus FE commercial software. Several cases of loading have been explored by varying the vertical load and the sliding velocity. The stress and strain fields are determined in steady-state regime. Numerical results give several cases of mechanical behavior: elasticity, elastic shakedown, plastic shakedown and ratcheting. Simulations are compared with the shakedown map results.

The different steel grades have been compared in terms of mechanical behavior for several levels of vertical loads and friction coefficients.

Concerning the risk of damage, the Crossland multiaxial fatigue criterion is proposed as a first step for the high cycle fatigue analysis in the case of elastic shakedown [3]. The results are analyzed in terms of level of in-phase and out-of-phase stress loading, hydrostatic pressure and shear stresses showing the limits of the Crossland post-treatment and the difficulties to identify an accurate fatigue criterion.

## 2. Wheel-rail contact FEA calculation

### *2.1. Asymptotic loading paths and shakedown concept*

Three main types of fatigue damage due to rolling contact can be generally obtained depending of the wheel load and friction coefficient. With a heavy load and high friction coefficient, the damage initiation is generally located on the tread surface due to high plastic deformations and at the opposite, normal loads and low friction coefficient lead to sub-surface fatigue crack initiation mostly due to the influence of the local load hydrostatic pressure and the shear stress. In order to identify the type of damage in rolling contact fatigue (RCF), the shakedown map (figure 1, left) can be used, indicating the asymptotic behavior of structure under a contact pressure depending on the load level and the friction coefficient. This type of diagram has been proposed since many years by Johnson [4] and was more recently given by Ekberg [1] to predict the fatigue behavior of railway wheel material.

These diagrams are based on Hertz hypothesis and contact modeling. In Y-coordinate, one finds the vertical adimensional standardized load, which takes into account the geometry of the wheel and the rail, the force applied to the wheel and the constitutive material. In X-coordinate, one finds the friction coefficient between the wheel and the rail. Note that the shakedown map is derived under the assumption of full slip.

Several zones are identified in this diagram and they correspond to different local asymptotic behavior in the wheel depending on different conditions (load, dimensions, material) as well as the place of tiredness (on the surface or under surface). These asymptotic behaviors can be of four different natures (figure 1, right):

- Elastic behavior (a).
- Elastic shakedown: the material initially plasticizes but its behavior becomes again elastic after some cycles (b).
- Plastic shakedown: if the loading increases, the material plasticizes until a cyclic plastic state, i.e. a stabilization of its behavior with a constant cyclic variation of plastic deformations (c).
- Ratcheting: if the loading is further increased, the behavior is identical to that of plastic shakedown but is no more stable. There is thus accumulation of plastic deformations which quickly will generate the ruin of the material (d).

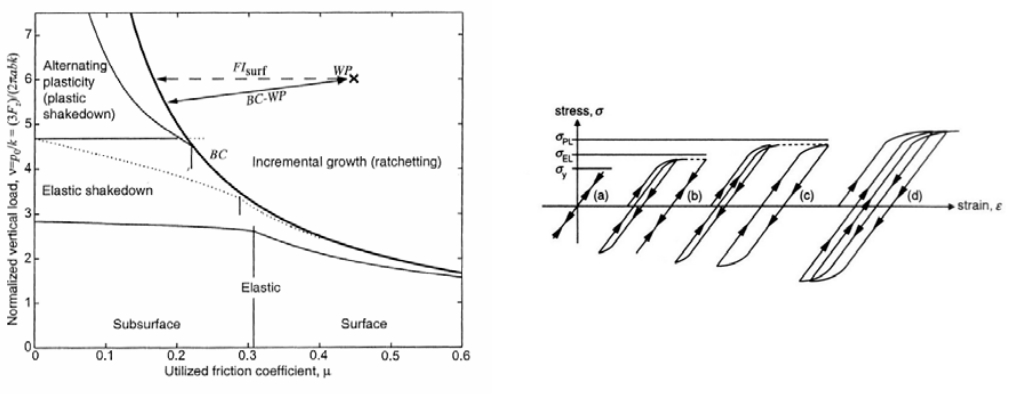


Fig. 1. on the left, example of Shakedown Map and, on the right, four different asymptotic states under cyclic loadings.

However, as the shakedown map only depends on the yield stress of the material, no more information is available about the hardening stress component and the plastic strain level which are necessary to determine a precise lifetime. The influence of different steel grades cannot be also properly taken into account.

### *2.2. Finite Element analysis*

In order to determine precisely the local loadings induced by the wheel-rail contact, a specific methodology has been developed which is able to evaluate the steel grades influence according to practical conditions. The main stages are the choice of a material constitutive law, the calibration of its parameters, the determination of the local stress-strain paths by using FEA and the application of the fatigue criterion. Such approach needs to get a precise estimation of the wheel/rail contact pressure and stresses highly depending on the material modeling. Two steel grades are considered in this paper, noted R9T and 50CrMo4.

#### *2.2.1. Constitutive law*

In order to realize mechanical tests for the characterization of the material mechanical behavior, different steel grades specimens were extracted from the tread wheel subjected to heat treatment. Cyclic strain controlled tensile-compressive tests were first performed on specimens at different strain amplitudes, from 0.1% to 1.2%. Fifty cycles were carried out for each strain amplitude in order to obtain a quasi-stabilized response of the material. The stabilized responses during such mechanical cyclic tests are presented in figure 2 (left) for the R9T steel. By considering the stabilized response obtained for a 2% strain amplitude on the maximal stress level (see figure 2, right), one can observe a small difference between both steels and the main objective of the work consists in the analysis of the influence of this difference on the local response of the wheel. Moreover, the obtained stress-strain curves exhibits an elastoplastic behavior essentially associated with a purely kinematic-type hardening.

Therefore, the non linear kinematic hardening model of Armstrong-Frederick was chosen [5], associated to a von Mises type plastic criterion $f$ :

$$f = J_2\left(\underline{\underline{A}}\right) - k \text{ where } J_2\left(\underline{\underline{A}}\right) = \sqrt{\frac{3}{2}\underline{\underline{A}} : \underline{\underline{A}}} \text{ and } \underline{\underline{A}} = dev\left(\underline{\underline{\sigma}}\right) - \underline{\underline{X}}.$$

The constant $k$ is the tensile yield stress, considered here as a constant and $\underline{\underline{X}}$ is the hardening back stress defined as:

$$\dot{\underline{\underline{X}}} = \frac{2}{3} C \dot{\underline{\underline{\alpha}}} \quad with \quad \dot{\underline{\underline{\alpha}}} = \dot{\underline{\underline{\varepsilon}}}_p - \frac{3}{2}\frac{\gamma}{C}\underline{\underline{X}}\dot{p} \quad and \quad p = \int_0^t \sqrt{\frac{2}{3}\dot{\underline{\underline{\varepsilon}}}_p : \dot{\underline{\underline{\varepsilon}}}_p}\, dt$$

where $C$ and $\gamma$ are the hardening parameters and $p$ is the cumulated plastic strain.

The four parameters of this model (the Young modulus, the yield limit and the two hardening parameters) are then identified from the stabilized stress-strain curves (figure 2, right) by minimizing the gap between experimental and simulated stresses.

As the Armstrong-Frederick model is available in the Abaqus commercial FE code, the parameters are just to be precise. As an example, a comparison between the experimental hardening curve and the Armstrong-Frederick model is presented on Figure 3 for the R9T steel.

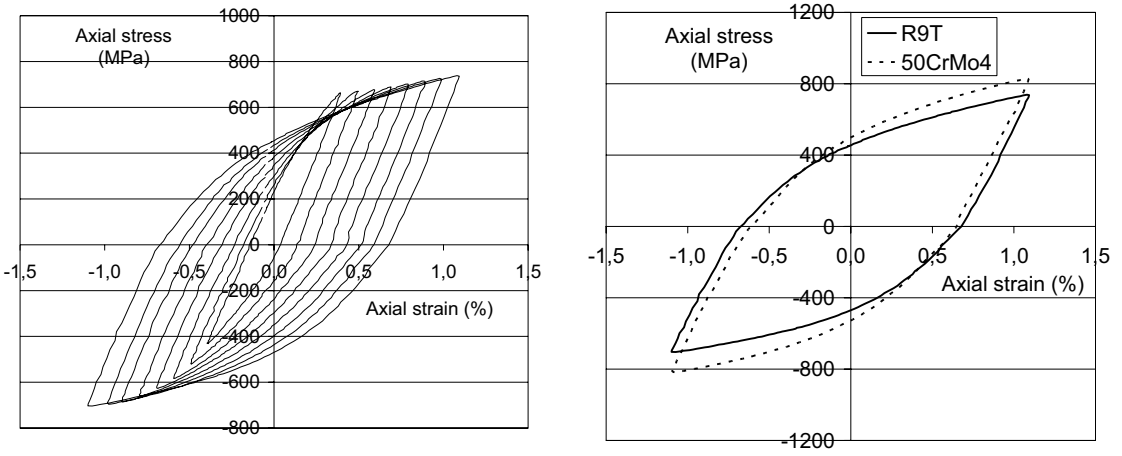


Fig. 2 on the left, stabilized stress-strain curve for different strain amplitudes for the R9T steel and, on the right, comparison of the stabilized stress-strain curves for a 2% strain amplitude for the two steels: R9T and 50CrMo4.

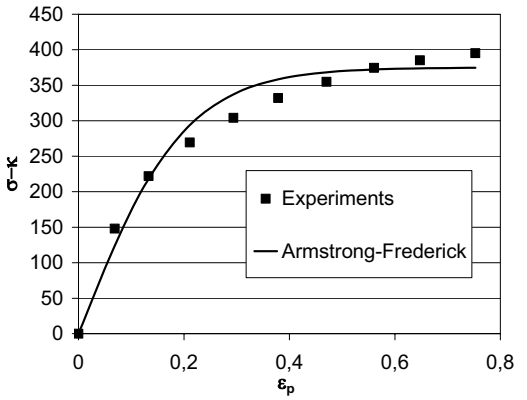


Fig. 3. comparison between the experimental hardening curve and the Armstrong-Frederick model for the R9T steel.

*2.2.2. Numerical model of the wheel-rail contact*

Modeling rolling and sliding contact of a railway wheel along the rail using a traditional Lagrangian formulation is computationally very expensive since a transient analysis must be performed. With such an incremental resolution, fine meshing is required along the entire surface of the wheel and also on the rail and several revolutions have to be simulated to obtain the stabilized solution due to successive loading (one at each revolution). In order to reduce computing time, we propose to adopt a steady-state Eulerian description using a reference frame that is attached to the axle of the rotating wheel, leading to a fine mesh only near the contact zone [2]. The analysis was

carried out with Abaqus software with the steady-state transport analysis capability. The steady-state transport analysis requires the definition of streamlines, which are the trajectories that the material follows during transport through the mesh. For the wheel-rail contact, the wheel is treated with the Eulerian method while the rail is treated with the Lagrangian method.

The 3D-model is created by revolving an axisymmetric model of the wheel about its axis of revolution and is presented in Figure 4, on the left. The inner radius of the railway wheel is clamped and the normal load is applied on the foot of the rail. The spinning motion of the wheel around its axis and the translation motion of the wheel with respect to the rail may be defined to model the sliding between the two deformable bodies (the wheel and the rail) that are moving with different velocities. The friction model used is a classical Coulomb friction law.

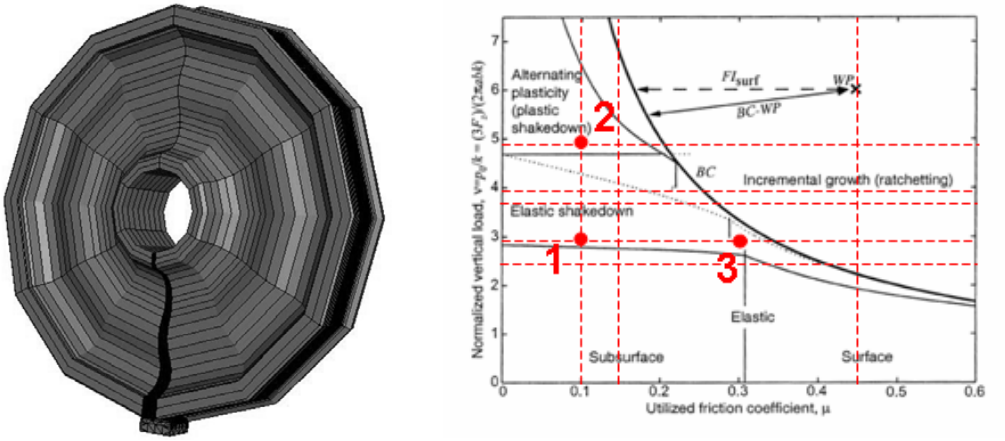


Fig. 4. on the left, FE model of the wheel rail contact in the case of the Eulerian approach and, on the right, three considered loading cases on the shakedown map: elastic shakedown for different friction coefficient (cases 1 and 3) and plastic shakedown (case 2).

## 3. Results

### *3.1. Stress and strain fields on the wheel*

Several configurations have been computed. Corresponding cases are located on the shakedown map in figure 4, on the right, in terms of vertical loading and friction coefficient between the wheel and the rail.. As a first case, the wheel load is around 30 kN (30723 N) and the friction coefficient is 0.1 corresponding to case 1. In a first step, for sake of simplicity, no sliding was considered between the wheel relative to the rail.

Some features of the steady-state response to this loading condition are visualized in Figure 5 in terms of von Mises equivalent stress and shear stress obtained by the FE simulation for the R9T steel grade.

The maximal von Mises equivalent stress is located at the sub surface and is around 580 MPa. The shear stress is also maximal in sub surface at 2 mm depth under the wheel tread, which is in accordance with the shakedown map. The stress concentrations around the contact area are evident by the visualization of the above-mentioned stress contour plot.

In the following, local stress-strain responses will be considered on a streamline situated at the maximum shear stress area. As described in section 2.2.2., by considering an eulerian approach, the analysis of a streamline corresponds to the analysis of the mechanical response during one cycle.

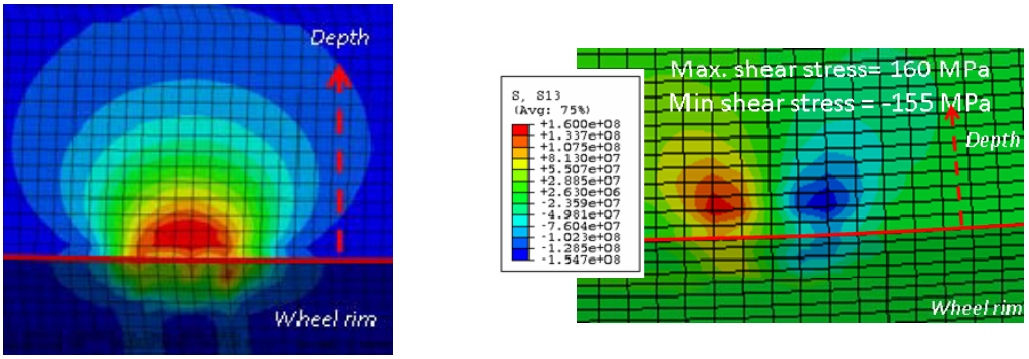


Fig. 5. on the left, von Mises stress distribution in the depth of the wheel, in the contact area for a 30273 N axial load and, on the right, shear stress distribution in the depth of the wheel, in the contact area for a 30273 N axial load (case 1)

### *3.2. Local stress-strain response*

Case 1 corresponds to a wheel load around 30 kN and a friction coefficient of 0.1, without considering sliding. The local stress-strain response obtained on the streamline passing through the maximum shear stress area is presented in Figure 6, on the left, for both steels, R9T and 50CrMo4. One can observe an elastic shakedown state for the 50CrMo4 steel and a quite close response for the R9T with a lower variation of the plastic deformation. Elastic shakedown is indicated by the shakedown map (Figure 4) but without differencing materials. Here we can notice a small difference between both responses which indicates an influence of the steel elastoplastic behavior. This difference increases in Figure 6, on the right, for a higher loading of around 137 kN. In this case, as the asymptotic response remains quite elastic for the 50CrMo4 steel, a plastic shakedown state is obtained with the R9T. This shows the important sensitivity of the proposed numerical method to the steel grade.

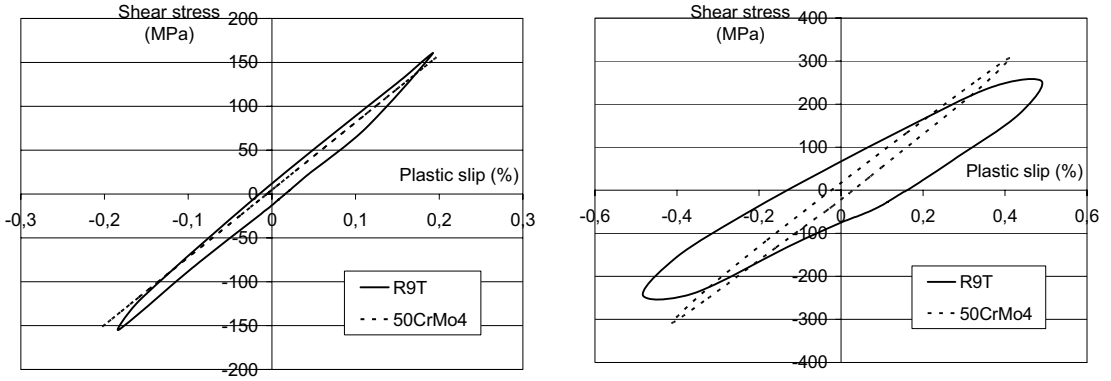


Figure 6: on the left, local stress-strain response obtained on a streamline situated in the maximum shear stress area for a load of 30273 N and a friction coefficient of 0.1, without sliding (case 1 on Figure 4) and, on the right, for a 136782 N loading and a 0.1 friction coefficient, without sliding (case 2 of Figure 4).

The last point concerns the influence of the friction coefficient. A comparison is done for a load of around 30kN, with sliding conditions and two friction coefficients, 0.1 and 0.3. This corresponds to cases 1 and 3 in Figure 4, with sliding. The obtained responses for the R9T steel are presented in Figure 7.

As it can be observed in Figure 7, the first impact of the friction coefficient is the translation of the maximum

shear stress zone from the subsurface to the surface. It is illustrated on the shakedown map in figure 4 by a translation of point 1 to point 3, from the zone called subsurface to the one called surface. One can also see differences in the shear distribution with and without sliding by comparing figure 5 and figure 7 on the top in the case of a 0.1 friction coefficient. With sliding the dissymmetry of shear stresses relative to the contact zone increases with a maximal value moving slightly to the surface.

Figure 7 presents also the local stress-strain response on the point of maximal shear stress with the two friction coefficients in the case of the R9T steel. Globally the behavior remains closed to elastic shakedown with low variations of the plastic deformation. The friction coefficient has mainly an influence on the mean strain with a lower impact on the mean stress. This can have some consequence in the fatigue analysis which is presented in the next section.

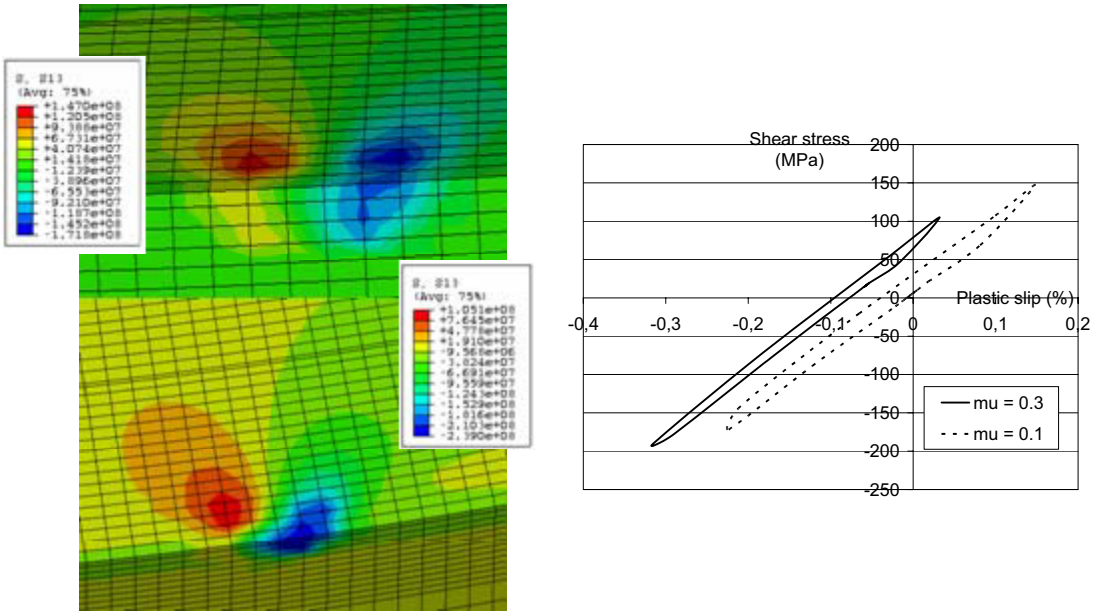


Fig. 7. on the left, shear stress distribution for two friction coefficients (0.1 on the top and 0.3 on the bottom) with sliding. Normal load is 30273 N (case 1 and 3) and, on the right, local stress-strain response obtained on a streamline situated in the maximum shear stress area for a load of 30273 N with sliding condition and a friction coefficient of 0.1 and 0.3 (case 1 and 3 of Figure 4), for the R9T steel.

### *3.3. Fatigue analysis*

The two main behavior types corresponding to elastic and plastic shakedown can be associated to low cycle fatigue in the first case and high cycle fatigue in the second case. In the case of high cycle fatigue, many multiaxial fatigue criteria have been developed, particularly since the 50's. One of the first one was certainly the Crossland criterion [3]. It combines linearly the amplitude of the second invariant of the deviatoric part of the stress tensor, denoted $\sqrt{J_2}_a$ and the maximal hydrostatic pressure during the cycle, $P_{\max}$:

$$\sqrt{J_2}_a + \alpha P_{\max} < \beta$$

where:

$$\begin{cases} \alpha = \dfrac{t - \dfrac{f}{\sqrt{3}}}{\dfrac{f}{3}} \\ \beta = t \end{cases}$$

with $f$ the fatigue limit in flexion and $t$, the fatigue limit in torsion. The main difficulty is the determination of $\sqrt{J_2}_a$ for arbitrary loading paths. However, one can show that:

$$\sqrt{J_2}_a = \frac{D}{2\sqrt{2}}$$

where $D$ is the diameter of the smallest hypersphere circumscribed to the loading path in the deviatoric stress space. This diameter can be determined by min-max procedures [6].

The Crossland criterion has been successfully applied in the cases where elastic shakedown is determined. However the principal difficulty of a high cycle fatigue analysis is the out-of-phase character of the rolling contact loading, in particular between normal and shear components, with large mean stress. This is illustrated in figure 8 showing relations between components of the stress tensor. It shows that loading are mainly non proportional with out-of-phase evolutions. This aspect has been also already pointed out by Bernasconi et al. [7] and has to be more particularly studied.

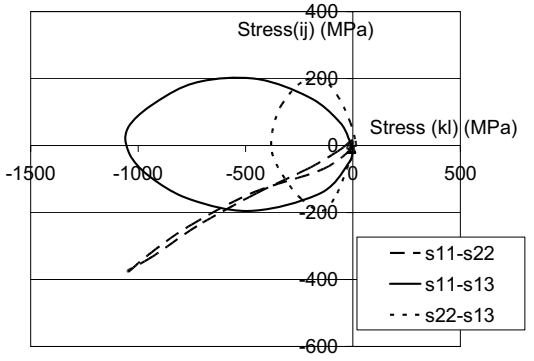


Fig. 8. in-phase and out-of-phase loading paths in the maximum shear stress area for the R9T steel. Out-of-phase paths are more particularly observed between normal and shear components

## 4. Conclusion

A numerical methodology for the analysis of rolling contact fatigue of railways wheels has been proposed in this paper. The main stages are the identification of the material behavior, the determination of the stress-strain fields and the analysis of stresses for the choice of a fatigue criterion. The behavior of materials has been characterized with tension-compression cyclic tests and modeled with a kinematic hardening. The numerical model uses a eulerian analysis reducing computing time compared to a transient resolution. Two steels usually used for the manufacturing of wheels have been studied, R9T and 50CrMo4, and their influence on the stress-strain stabilized response has been numerically studied. Results show high differences of cyclic behavior in the case of high loading with plastic shakedown for the R9T steel as it remains close to elastic shakedown for the 50CrMo4 steel. The effect of sliding is

also shown.

This approach enables to take into account the elastoplastic characteristics of the different steels considered by using a non-linear hardening model. This first case seems to give consistent results with respect to the shakedown map. Moreover, a local response is available which enables the use of a fatigue criterion for the evaluation of the vicinity of the loading path. However, it can be noticed that out-of-phase loadings with large mean stress are obtained which are very difficult to analyse with conventional fatigue criteria, especially in the case of high cycle fatigue. Further works are devoted on that point.

## References

[1] A. Ekberg and E. Kabo, Wear, vol. 258, 2005, pp. 1288-1300.

[2] K. Dang Van and M.H. Maïtournam, J. Mech. Phys. Solids, vol. 41, iss. 11, 1993, pp. 1691-1710.

[3] B. Crossland, Proc. Int. Conf. Fatigue of Metals, Inst. Mech. Engng., 1956, pp. 138-149.

[4] K.L. Johnson, Contact Mechanics, Cambridge University Press, 1985.

[5] P.J. Armstrong and C.O. Frederick, Technical Report RD/B/N731, Berkeley Nuclear Laboratories, 1966.

[6] K. Dang-Van and I. Papadopoulos., High cycle metal fatigue – from theory to applications, Springer-Verlag, 1999.

[7] A. Bernasconi, M. Filippini, S. Foletti and D. Vaudo, Int. J. Fat., vol. 28, 2006, pp. 663–672.